



# EL2425 – Automatic Control, Project Course

## Slip Control

January 5, 2017

Final report

Alexandros Filotheou, Melih Guldogus, Tengfan Lin,  
Roberto Sanchez-Rey, Xuechun Xu

# Contents

1	Introduction	3
2	Documentation resources	3
3	Tracking the centerline of a lane using a PID controller	4
3.1	Theoretical approach to solution . . . . .	4
3.1.1	Translational component . . . . .	4
3.1.2	Rotational component . . . . .	5
3.2	Experimental results . . . . .	8
4	Tracking the centerline of a lane using a MPC controller	10
4.1	Theoretical approach to solution . . . . .	10
4.1.1	Initial conditions . . . . .	10
4.1.2	Obtaining the linearized kinematic model . . . . .	13
4.1.3	Stating the optimization problem . . . . .	15
4.2	Experimental results . . . . .	15
5	Tracking the circumference of a circle using a MPC controller	17
5.1	Theoretical approach to solution . . . . .	17
5.1.1	Finding $T$ . . . . .	18
5.1.2	Beyond point $T$ . . . . .	19
5.1.3	Obtaining the linearized kinematic model . . . . .	20
5.1.4	Stating the optimization problem . . . . .	22
5.2	Experimental results . . . . .	22
6	On the dynamic model	26
6.1	Dynamic model equations . . . . .	26
6.2	Parameter estimation . . . . .	27
7	Conclusion	28

# 1 Introduction

This report summarizes the work done by a group of students, namely Alexandros Filotheou, Melih Guldogus, Tengfan Lin, Roberto Sanchez-Rey and Xuechun Xu, at KTH under EL2425 - Automatic Control Project Course, during the winter semester of 2016.

In it, we include the theoretical approaches to the solution of three problems, and their respective experimental performance and results. These problems pertain to the control of the behaviour of a F1/10 RC car: directing and maintaining the trajectory of the vehicle at the centerline of a virtual lane using PID and predictive control, and directing and maintaining the trajectory of the vehicle on the circumference of a circle using predictive control.

# 2 Documentation resources

The progress of the project is documented in trello and github:

- <https://trello.com/b/uEP0jl0B/slip-control>
- [https://gits-15.sys.kth.se/alefil/HT16\\_P2\\_EL2425](https://gits-15.sys.kth.se/alefil/HT16_P2_EL2425)
- [https://gits-15.sys.kth.se/alefil/HT16\\_P2\\_EL2425\\_resources](https://gits-15.sys.kth.se/alefil/HT16_P2_EL2425_resources)



The angular error of the translational component is then

$$e_t = -\tan^{-1} \frac{CL - CR}{2CC'} \quad (4)$$

where the minus sign is introduced due to the convention that a left turn is assigned a negative value.

### 3.1.2 Rotational component

The rotational component problem can be solved in two ways, of which the second is more robust than the first.

In the first solution, we assume that the the pose of the vehicle at time  $t$  as  $(x_c, y_c, v_c, \psi_v)$  and that three range scans at  $+90^\circ$ ,  $0^\circ$  and  $-90^\circ$  with respect to the longitudinal axis of the vehicle are available, which are denoted as  $CL$ ,  $CF$  and  $CR$  respectively.

Here we can distinguish two cases: one where the vehicle is facing the right lane boundary and one where it is facing the left one. It is not obvious in this configuration where the vehicle is heading: the only available information so far is only the three range scans.

In the first case, the heading angle error is

$$\phi = \tan^{-1} \frac{CR}{CF} \quad (5)$$

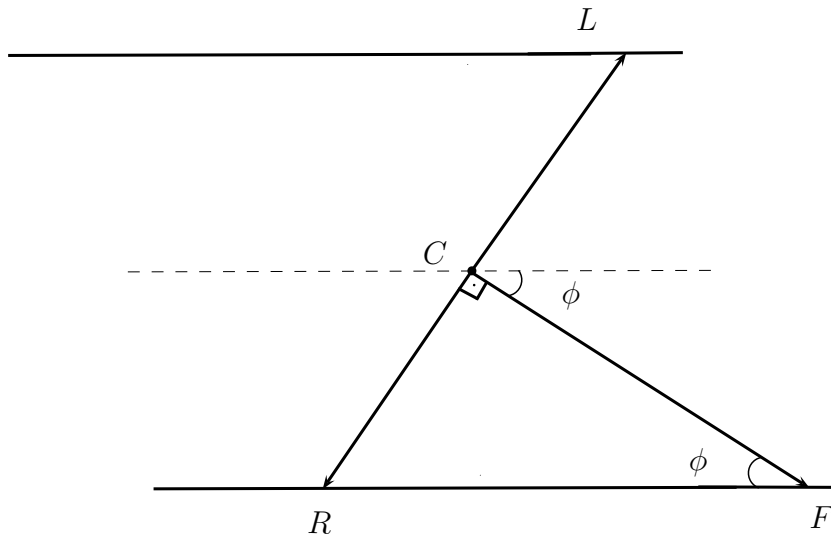


Figure 2: The vehicle's position and its reference are equal. However, the vehicle's heading is off track. Its heading is towards the right lane boundary.

The rotational error of the vehicle in this case is

$$e_r = -\tan^{-1} \frac{CR}{CF} \quad (6)$$

therefore the overall angular error of the vehicle in this case is

$$e = -\tan^{-1}\frac{CL - CR}{2CC'} - \tan^{-1}\frac{CR}{CF} \quad (7)$$

where the minus signs are introduced due to the convention that a left turn is assigned a negative value.

In the second case, the heading angle error is

$$\phi = \tan^{-1}\frac{CL}{CF} \quad (8)$$

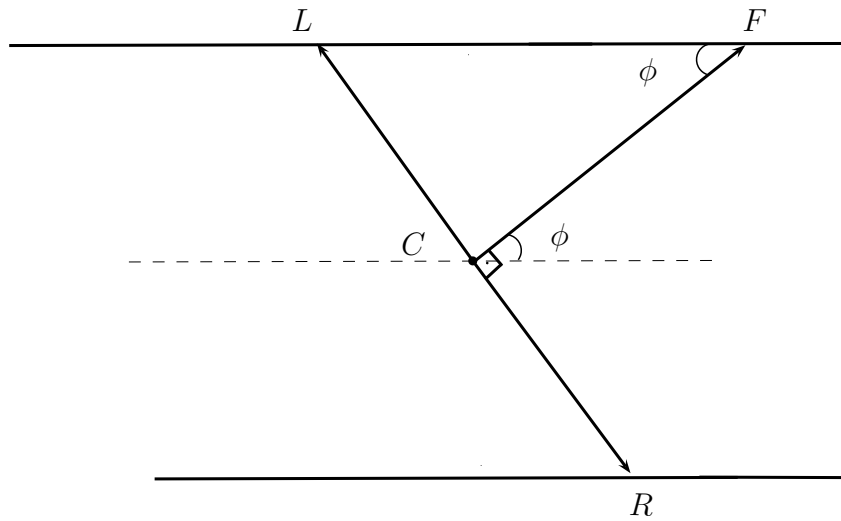


Figure 3: The vehicle's position and its reference are equal. However, the vehicle's heading is off track. Its heading is towards the left lane boundary.

The rotational error of the vehicle in this case is

$$e_r = \tan^{-1}\frac{CL}{CF} \quad (9)$$

therefore the overall angular error of the vehicle in this case is

$$e = -\tan^{-1}\frac{CL - CR}{2CC'} + \tan^{-1}\frac{CL}{CF} \quad (10)$$

where the minus sign of the translational error is introduced due to the convention that a left turn is assigned a negative value.

In order to deduce the correct value of  $\phi$  ( $-\tan^{-1}\frac{CR}{CF}$  or  $\tan^{-1}\frac{CL}{CF}$ ) further range scans are needed. To this end, a difference between ranges around point  $F$  is taken: starting at the right of  $F$  and moving anti-clockwise, we calculate the difference between two range scans for a given angle between them. If its sign is negative then the vehicle is facing the right lane boundary; if not, it is facing the left lane boundary. This concept is depicted in figures 4 and 5.

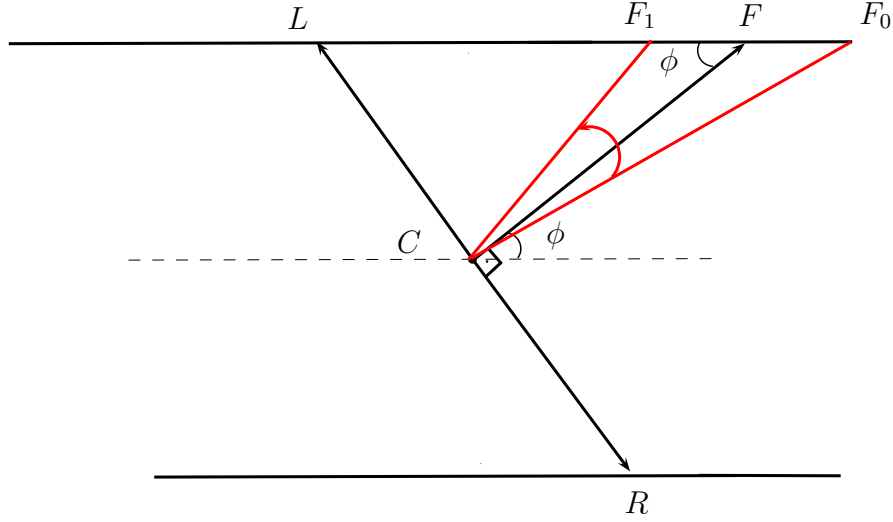


Figure 4:  $CF_0 > CF > CF_1$ , hence  $CF_0 - CF_1 > 0$  and  $\phi = \tan^{-1} \frac{CL}{CF}$

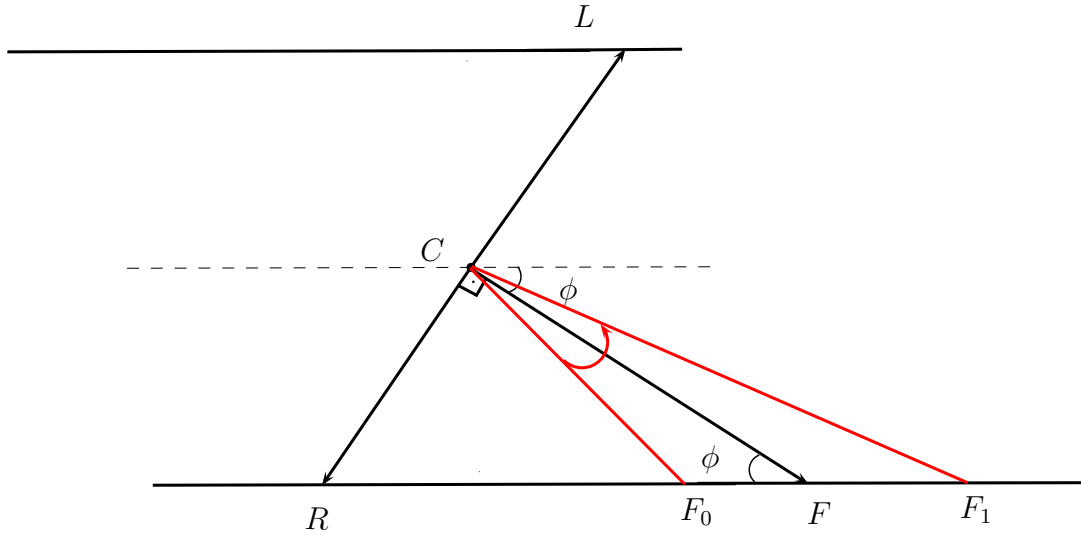


Figure 5:  $CF_0 < CF < CF_1$ , hence  $CF_0 - CF_1 < 0$  and  $\phi = -\tan^{-1} \frac{CR}{CF}$

In the second solution we assume that the the pose of the vehicle at time  $t$  as  $(x_c, y_c, v_c, \psi_v)$  and that two range scans at  $+90^\circ$  and  $-90^\circ$  with respect to the longitudinal axis of the vehicle are available, which are denoted as  $CL$  and  $CR$  respectively. Here, again we distinguish two cases, one where the vehicle is facing the right lane boundary and one where it is facing the left one. It is not obvious in this configuration where the vehicle is heading: the only available information so far is only the two ranges  $CR$  and  $CL$ .

We retrieve the first minimum distance from the range scan available at time  $t$ , and denote the point which corresponds to this distance with  $M_0$ . The angle between point  $M_0$  and the longitudinal axis of the vehicle is denoted with  $\alpha$ . In order to find this angle, we can exploit the fact that each ray of the scan is separated from the next by  $res$  degrees, while all of them are stored in an array sequentially, in an anti-clockwise manner. In the case of the HOKUYO-UST-10LX-LASER, the angular resolution is  $res = 0.25^\circ$ , and the

starting angle is  $-135^\circ$  with respect to the longitudinal axis of the vehicle. This means that we can retrieve the angle  $\alpha$  by first calculating the number of indices between the one that corresponds to the ray with the minimum range and the one that corresponds to  $+135^\circ$  (which in our case is  $135/0.25 = 540$ ) with regard to the laser's system of reference, and then by multiplying this number  $\Delta i$  by the angular resolution  $res$ . Hence,  $\alpha = 0.25 \times \Delta i$ .

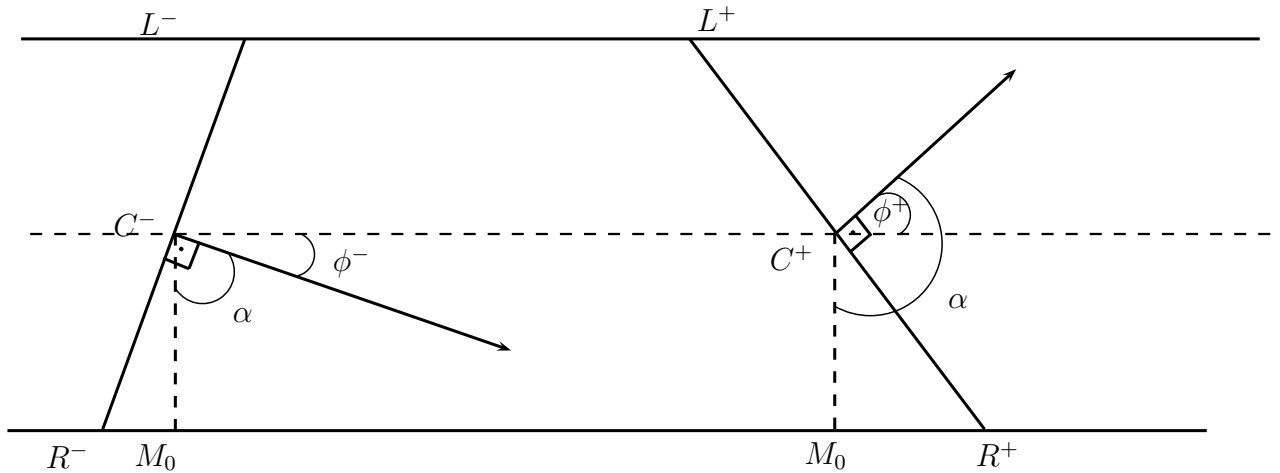


Figure 6

At this point we do not know whether the vehicle is pointing to the left or to the right lane boundary yet. However, we can determine the sign and the magnitude of the orientation of the vehicle with respect to the orientation of the lane by examining the sign of the difference  $\alpha - 90^\circ$ : if it is negative, the vehicle is pointing towards the right boundary lane, if it is positive, towards the left. Furthermore, we can now calculate the magnitude of the orientation of the vehicle as the difference  $|\alpha - 90^\circ|$ , as shown in figure 12. In conclusion, when the car is located at the centerline, its orientation with respect to the orientation of the lane is

$$\phi = \alpha - 90^\circ$$

therefore the overall angular error of the vehicle in this case is

$$e = -\tan^{-1} \frac{CL - CR}{2CC'} + \alpha - 90 \quad (11)$$

Since the input to the plant is in terms of angular displacement, this is in fact the error that the PID controller can include and utilize in order to determine the plant's input.

The angular input to the vehicle will then be

$$\delta = K_p \cdot e + K_d \cdot \frac{de}{dt} + K_i \cdot \int e dt \quad (12)$$

### 3.2 Experimental results

Here, we opted for the second solution, due to its simplicity and robustness in comparison to the first one. After tuning, the gains were determined as such:



$$K_p = 0.7$$

$$K_d = 0.1$$

$$K_i = 0.003$$

and  $CC'$  was set to  $CC' = 3.0$ . Figures 7 and 8 illustrate the compound angular error and the input steering angle through time, when the initial orientation of the vehicle is positive. Figures 9 and 10 illustrate the compound angular error and the input steering angle through time for two distinct experiments, when the initial orientation of the vehicle is positive and negative respectively.

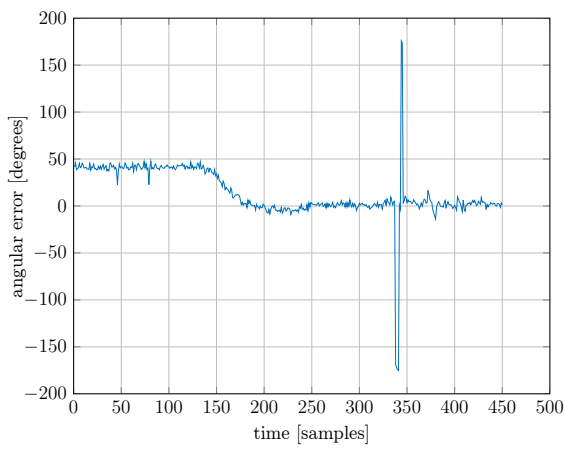


Figure 7: The composite angular error. Initial orientation is positive.

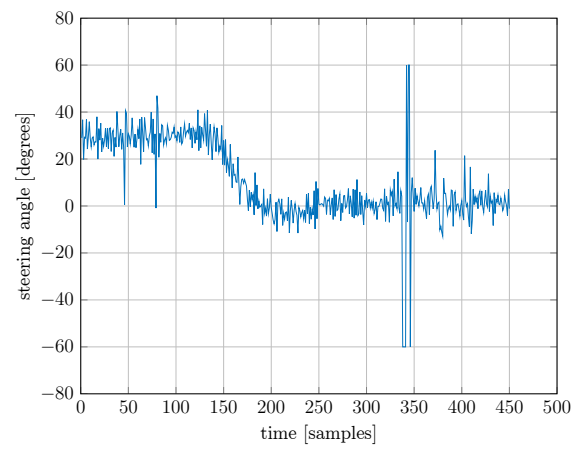


Figure 8: The input steering angle. Initial orientation is positive.

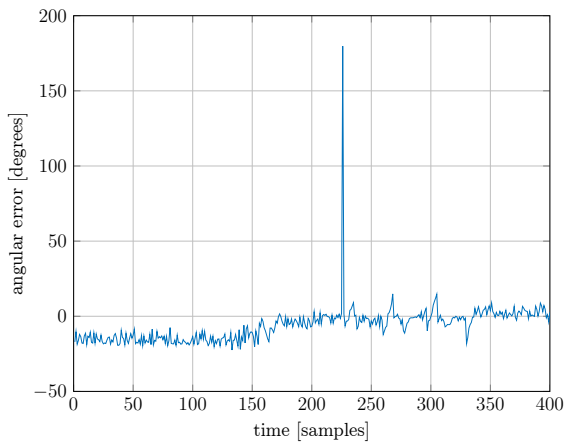


Figure 9: The composite angular error. Initial orientation is negative.

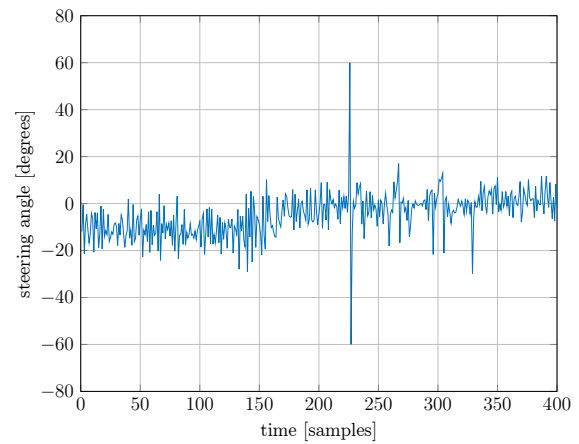


Figure 10: The input steering angle. Initial orientation is negative.

The PID controller makes the vehicle quick in its reaction, and can successfully position it in the middle of the lane. However, it is susceptible to even minute disturbances.

## 4 Tracking the centerline of a lane using a MPC controller

### 4.1 Theoretical approach to solution

In figure 11, the  $x$  axis is fixed on the lane's centerline, while axis  $y$  is perpendicular to it, facing the left boundary of the lane. The origin is at point  $O$ . The vehicle is represented by point  $C$ . The orientation of the vehicle with respect to the lane (the  $x$ -axis) is  $\phi$ . Given this configuration and two ranges from the range scan, at  $-90^\circ$  and  $90^\circ$  with respect to the longitudinal axis of the vehicle (denoted by  $CR$  and  $CL$  respectively), the objective is to find the distance  $OC$  and the angle  $\phi$  so that a MPC optimization problem can be solved with  $OC$  and  $\phi$  acting as initial conditions. The only source of information is the lidar itself.

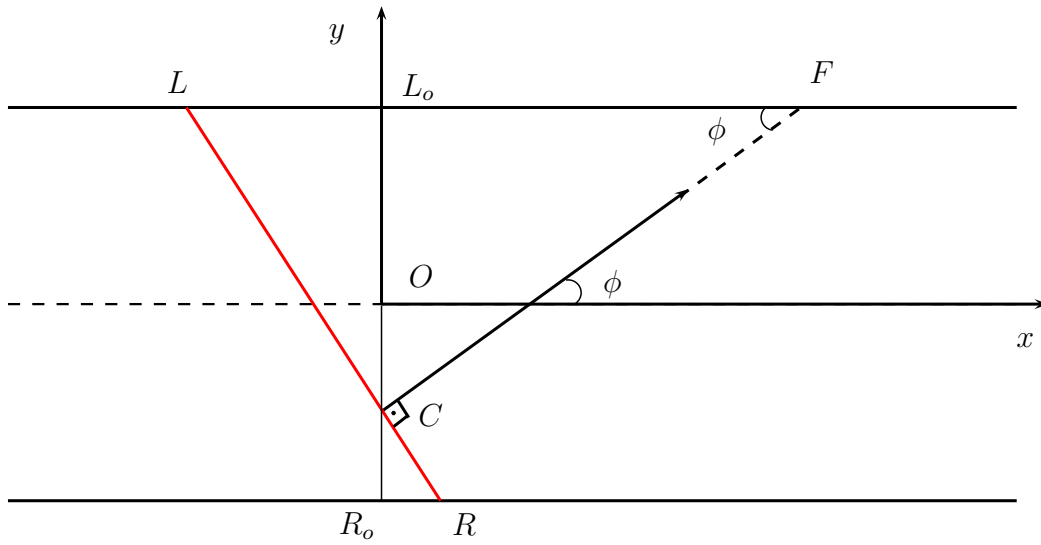


Figure 11

#### 4.1.1 Initial conditions

##### Finding $\phi$

Here we can distinguish two cases, one where the vehicle is facing the right lane boundary and one where it is facing the left one. It is not obvious in this configuration where the vehicle is heading: the only available information so far is only the two ranges  $CR$  and  $CL$ .

In the first case, when the vehicle is on the right semilane,  $CL - CR > 0$ . We retrieve the minimum distance from the range scan available at time  $t$ , and denote the point which corresponds to this distance with  $M$ . The angle between point  $M$  and the longitudinal axis of the vehicle is denoted with  $\alpha$ . In order to find this angle, we can exploit the fact that each ray of the scan is separated from the next by  $res$  degrees, while all of them are stored in an array sequentially, in an anti-clockwise manner. In the case of the HOKUYO-UST-10LX-LASER, the angular resolution is  $res = 0.25^\circ$ , and the starting angle is  $-135^\circ$  with respect to the longitudinal axis of the vehicle. This means that we can retrieve the angle  $\alpha$  by first calculating the number of indices between the one that corresponds to the ray with the minimum range and the one that corresponds to  $+135^\circ$  (which in our case is  $135/0.25 = 540$ ) with regard to the laser's system of reference, and then by multiplying this number  $\Delta i$  by the angular resolution  $res$ . Hence,  $\alpha = 0.25 \times \Delta i$ .

At this point we do not know whether the vehicle is pointing to the left or to the right lane boundary. However, we can determine the sign and the magnitude of the orientation of the vehicle with respect to the orientation of the lane by examining the sign of the difference  $\alpha - 90^\circ$ : if it is negative, the vehicle is pointing towards the right boundary lane, if it is positive, towards the left. Furthermore, we can now calculate the magnitude of the orientation of the vehicle as the difference  $|\alpha - 90^\circ|$ , as shown in figure 12. In conclusion, if the car is located at the right semilane its orientation with respect to the orientation of the lane is

$$\phi = \text{sign}(CL - CR)(\alpha - 90)$$

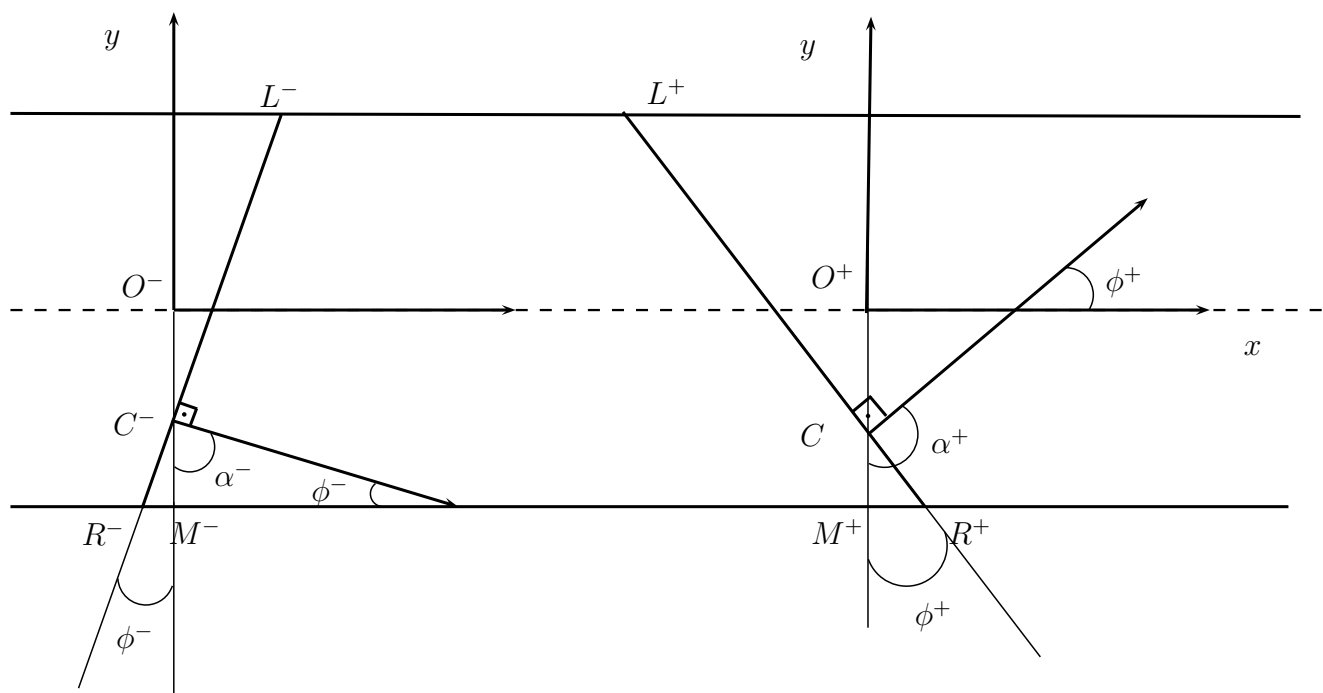


Figure 12: The vehicle is at the right side of the lane.

In the second case, when the vehicle is on the left semilane,  $CL - CR < 0$ . We retrieve the minimum distance from the range scan available at time  $t$ , and denote the point which corresponds to this distance with  $M$ . The angle between point  $M$  and the longitudinal axis of the vehicle is denoted with  $\alpha$ . In order to find this angle, we can exploit the fact that each ray of the scan is separated from the next by  $res$  degrees, while all of them are stored in an array sequentially, in an anti-clockwise manner. In the case of the HOKUYO-UST-10LX-LASER, the angular resolution is  $res = 0.25^\circ$ , and the starting angle is  $-135^\circ$  with respect to the longitudinal axis of the vehicle. This means that we can retrieve the angle  $\alpha$  by first calculating the number of indices between the one that corresponds to the ray with the minimum range and the one that corresponds to  $+225^\circ$  (which in our case is  $225/0.25 = 900$ ) with regard to the laser's system of reference, and then by multiplying this number  $\Delta i$  by the angular resolution  $res$ . Hence,  $\alpha = 0.25 \times \Delta i$ .

At this point we do not know whether the vehicle is pointing to the left or to the right lane boundary. However, we can determine the sign and the magnitude of the orientation of the vehicle with respect to the orientation of the lane by examining the sign of the difference  $\alpha - 90^\circ$ : if it is positive, the vehicle is pointing towards the right

boundary lane, if it is negative, towards the left. Furthermore, we can now calculate the magnitude of the orientation of the vehicle as the difference  $|\alpha - 90^\circ|$ , as shown in figure 13. In conclusion, if the car is located at the left semilane its orientation with respect to the orientation of the lane is

$$\phi = \text{sign}(CL - CR)(\alpha - 90)$$

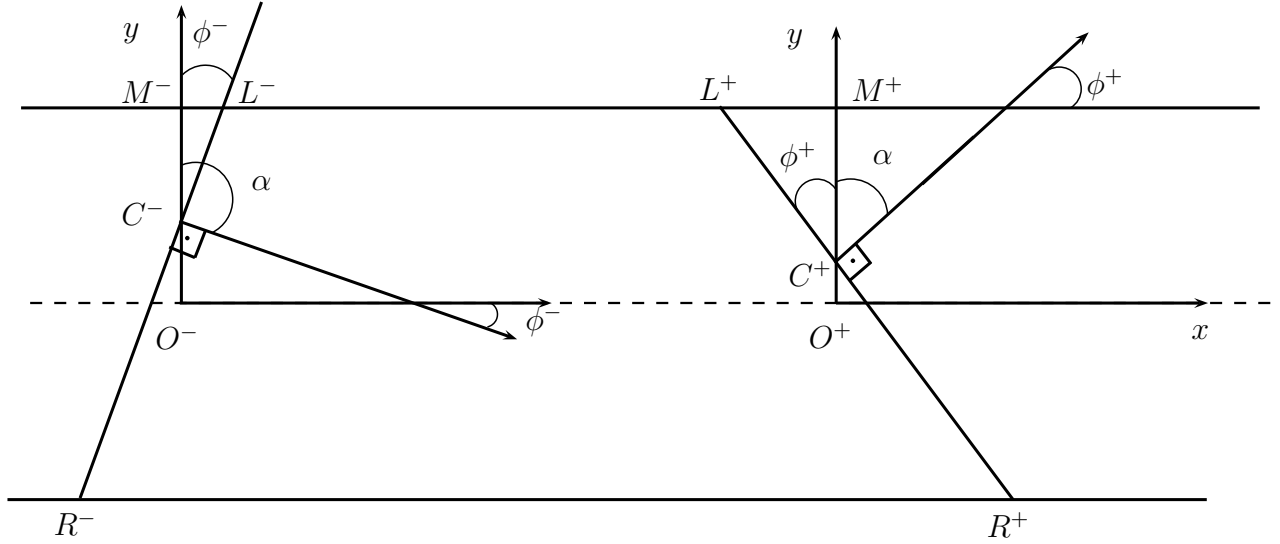


Figure 13: The vehicle is at the left side of the lane.

In conclusion, angle  $\phi = \text{sign}(CL - CR)(\alpha - 90)$ , where angle  $\alpha$  is calculated as a (weighted by angular resolution) difference between the indices of the minimum range provided by the range scan at time  $t$  and that of the minimum range between  $CL$  and  $CR$ .

#### Finding $OC$

Looking at figure 11 we can see that

$$L_oO + OC + CR_o = W = CR_o + CL_o \quad (13)$$

where  $W$  is the width of the lane. But  $L_oO = \frac{W}{2}$  hence

$$OC + CR_o = \frac{1}{2}(CR_o + CL_o) \Leftrightarrow \quad (14)$$

$$OC = \frac{1}{2}(CL_o - CR_o) \quad (15)$$

But  $CL_o = CL \sin \lambda$  and  $CR_o = CR \cos \phi$ , hence

$$OC = \frac{1}{2}(CL \sin \lambda - CR \cos \phi) \quad (16)$$

From triangle LCF in the case where the vehicle is facing the left lane boundary, we note that  $\phi + \lambda + \frac{\pi}{2} = \pi$ , hence  $\lambda = \frac{\pi}{2} - \phi$ . Then, we conclude that

$$OC = \frac{1}{2}(CL - CR) \cos \phi \quad (17)$$

#### 4.1.2 Obtaining the linearized kinematic model

The model constitutes the equations of motion of the vehicle, and has four states ( $x$ ,  $y$ ,  $v$  and  $\psi$ ), two inputs ( $v_i$  and  $\delta$ ) and the time constant  $\tau$ . The equations of the vehicle's motion that are relevant here are

$$\dot{x} = v \cos(\psi + \beta) \quad (18)$$

$$\dot{y} = v \sin(\psi + \beta) \quad (19)$$

$$\dot{v} = \frac{v_i - v}{\tau} \quad (20)$$

$$\dot{\psi} = \frac{v}{l_r} \sin \beta \quad (21)$$

For determining the value of  $\tau$ , with assumption that the car's dynamic is a 1st-order system, we drive the car in straight line along the Y axis(global) as far as possible with speed of 14%, 16%, 18% and 20% respectively. It is hard to reach the static situation since the space is limited, that is, the data only describe the beginning part of the step response. One way to solve the problem is using the Identification Toolbox in Matlab, which is capable of constructing mathematical models of dynamic systems from measured input-output data.

Through the identifications of experiments at 4 different velocity, the time constant can be caught by average

$$\tau = 1.01222s \quad (22)$$

And the maximum velocity of the car is

$$V_{max} = 13.56m/s \quad (23)$$

Regarding equations 18-21, sampling with a sampling time of  $T_s$  gives

$$x_{k+1} = x_k + T_s v_k \cos(\psi_k + \beta_k) \quad (24)$$

$$y_{k+1} = y_k + T_s v_k \sin(\psi_k + \beta_k) \quad (25)$$

$$v_{k+1} = v_k + \frac{T_s}{\tau} (v_{i,k} - v_k) \quad (26)$$

$$\psi_{k+1} = \psi_k + T_s \frac{v}{l_r} \sin \beta_k \quad (27)$$

where

$$\beta_k = \tan^{-1} \left( \frac{l_r}{l_r + l_f} \tan \delta_{k-1} \right) \quad (28)$$

Forming the Jacobians for matrices  $A$ ,  $B$  and evaluating them at time  $t = k$  around the state  $\psi = \phi$ ,  $v = v_k$  and  $\delta = \delta_{k-1}$  ( $\delta_k$  is to be determined at time  $k$ ):

$$A = \begin{bmatrix} 1 & 0 & T_s \cos(\phi + \beta_k) & -T_s v_k \sin(\phi + \beta_k) \\ 0 & 1 & T_s \sin(\phi + \beta_k) & T_s v_k \cos(\phi + \beta_k) \\ 0 & 0 & 1 - \frac{T_s}{\tau} & 0 \\ 0 & 0 & \frac{T_s}{l_r} \sin(\beta_k) & 1 \end{bmatrix} \quad (29)$$

$$A = \begin{bmatrix} 1 & 0 & T_s \cos\left(\phi + \tan^{-1}(l_q \tan \delta_{k-1})\right) & -T_s v_k \sin\left(\psi_k + \tan^{-1}(l_q \tan \delta_{k-1})\right) \\ 0 & 1 & T_s \sin\left(\phi + \tan^{-1}(l_q \tan \delta_{k-1})\right) & T_s v_k \cos\left(\psi_k + \tan^{-1}(l_q \tan \delta_{k-1})\right) \\ 0 & 0 & 1 - \frac{T_s}{\tau} & 0 \\ 0 & 0 & \frac{T_s}{l_r} \sin(\tan^{-1}(l_q \tan \delta_{k-1})) & 1 \end{bmatrix} \quad (30)$$

$$B = \begin{bmatrix} 0 & -T_s v_k \sin(\phi + \beta_k) \frac{l_q}{l_q^2 \sin^2 \delta_{k-1} + \cos^2 \delta_{k-1}} \\ 0 & T_s v_k \cos(\phi + \beta_k) \frac{l_q}{l_q^2 \sin^2 \delta_{k-1} + \cos^2 \delta_{k-1}} \\ \frac{T_s}{\tau} v_k & 0 \\ 0 & \frac{T_s v_k}{l_r} \cos(\beta_k) \frac{l_q}{l_q^2 \sin^2 \delta_{k-1} + \cos^2 \delta_{k-1}} \end{bmatrix} \quad (31)$$

$$B = \begin{bmatrix} 0 & -T_s v_k \sin\left(\phi + \tan^{-1}(l_q \tan \delta_{k-1})\right) \frac{l_q}{l_q^2 \sin^2 \delta_{k-1} + \cos^2 \delta_{k-1}} \\ 0 & T_s v_k \cos\left(\phi + \tan^{-1}(l_q \tan \delta_{k-1})\right) \frac{l_q}{l_q^2 \sin^2 \delta_{k-1} + \cos^2 \delta_{k-1}} \\ \frac{T_s}{\tau} v_k & 0 \\ 0 & \frac{T_s v_k}{l_r} \cos\left(\tan^{-1}(l_q \tan \delta_{k-1})\right) \frac{l_q}{l_q^2 \sin^2 \delta_{k-1} + \cos^2 \delta_{k-1}} \end{bmatrix} \quad (32)$$

where  $l_q = \frac{l_r}{l_r + l_f}$

Now we can express the linear model as

$$s_{k+1} = A s_k + B u_k \quad (33)$$

where

$$s_k = \begin{bmatrix} x_k \\ y_k \\ v_k \\ \psi_k \end{bmatrix}, u_k = \begin{bmatrix} v_{i,k} \\ \delta_k \end{bmatrix} \quad (34)$$

However, states  $x$  and  $v$  cannot be measured under our configuration, since no SLAM module is employed and no encoders are mounted on the wheels of the vehicle. Hence, the model has to be reduced, while now the velocity will be constant and set to  $v_0$ . (Hence the input throttle also needs to be excluded as an input). Nevertheless, state  $x$  needs to be included in the model even if it is not possible to measure it due to the formulation of the problem in terms of the MPC framework: the reference of the vehicle in terms of  $x$  needs to be (practical) infinity in order for it to keep moving along the lane. The new system matrices and the new states are modified as

$$A = \begin{bmatrix} 1 & 0 & -T_s v_k \sin(\psi_k + \tan^{-1}(l_q \tan \delta_{k-1})) \\ 0 & 1 & T_s v_k \cos(\psi_k + \tan^{-1}(l_q \tan \delta_{k-1})) \\ 0 & 0 & 1 \end{bmatrix} \quad (35)$$

$$B = \begin{bmatrix} -T_s v_k \sin(\phi + \tan^{-1}(l_q \tan \delta_{k-1})) \frac{l_q}{l_q^2 \sin^2 \delta_{k-1} + \cos^2 \delta_{k-1}} \\ T_s v_k \cos(\phi + \tan^{-1}(l_q \tan \delta_{k-1})) \frac{l_q}{l_q^2 \sin^2 \delta_{k-1} + \cos^2 \delta_{k-1}} \\ \frac{T_s v_k}{l_r} \cos(\tan^{-1}(l_q \tan \delta_{k-1})) \frac{l_q}{l_q^2 \sin^2 \delta_{k-1} + \cos^2 \delta_{k-1}} \end{bmatrix} \quad (36)$$

the model being

$$s_{k+1} = A s_k + B u_k, s_k = \begin{bmatrix} x_k \\ y_k \\ \psi_k \end{bmatrix}, u_k = [\delta_k] \quad (37)$$

#### 4.1.3 Stating the optimization problem

We can now form the optimization problem to be solved at time step  $t$  as

$$\text{minimize } \sum_{k=0}^{N-1} (s_k - s_{ref})^T Q (s_k - s_{ref}) + u_k^T R u_k + (s_N - s_{ref})^T Q_f (s_N - s_{ref}) \quad (38)$$

$$\text{subject to } s_{k+1} = A s_k + B u_k \quad (39)$$

$$\delta^{min} \leq \delta_k \leq \delta^{max} \quad (40)$$

$$s_0 = (x_t, y_t, \psi_t) \equiv (0, OC, \phi) \quad (41)$$

$$s_{ref} = (x^{max}, 0, 0) \quad (42)$$

$$Q > 0, R > 0, Q_f > 0 \quad (43)$$

## 4.2 Experimental results

We tested the performance of this functionality in the corridor that connects the buildings addressed as Osquidas vag 10 and 6.

The velocity of the vehicle was again kept at its minimum. The vehicle was positioned approximately one meter away from the centerline at the side of the negative  $y$  axis. Its

initial orientation with respect to the orientation of the centerline was  $-65^\circ$ , meaning that it begun facing the right-hand side wall.

With penalty matrices

$$Q = \begin{bmatrix} 1000 & 0 \\ 0 & 1200 \end{bmatrix}, R = 10000 \quad (44)$$

and a horizon length of  $N = 10$ , we plot the two main states of significance in figures 14 and 15: the displacement of the vehicle from the centerline and its orientation with respect to the orientation of the corridor itself. Figure 16 shows the steering angle that was given as input to the front wheels.

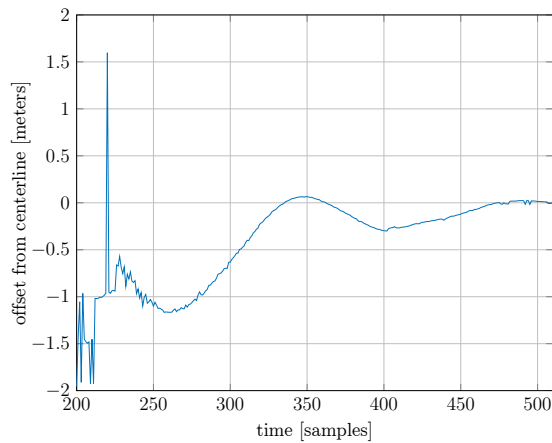


Figure 14: The displacement of the vehicle from the centerline in meters through time.

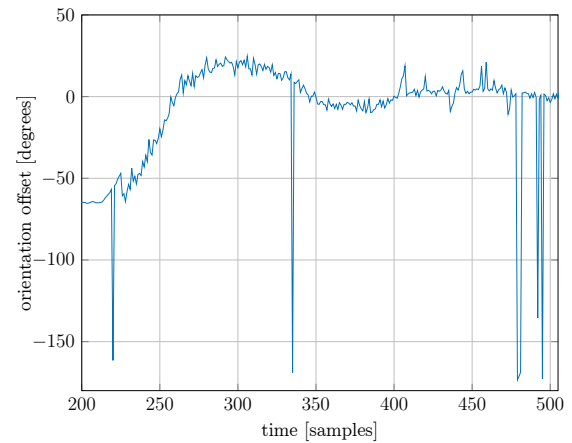


Figure 15: The orientation of the vehicle with respect to the orientation of the centerline through time.

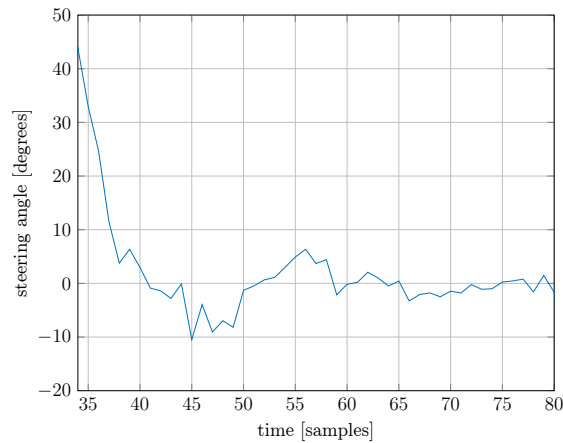


Figure 16: The steering angle given to the front wheels.

The vehicle succeeded in positioning itself in the centerline of the corridor. The displacement error is eliminated entirely by the end of the corridor, and the same applies for the vehicle's orientation.



## 5 Tracking the circumference of a circle using a MPC controller

### 5.1 Theoretical approach to solution

In figure 17, the vehicle  $C$ , whose velocity is constant and denoted by  $v$ , is to track a circle whose center is  $O'$  and whose radius is  $R$ . Its orientation relative to the global coordinate system is  $\psi$ . The vehicle's coordinates are  $(x_c, y_c)$ . The circular trajectory is known a priori, and is comprised of a set of ordered points who encode the  $x$ -wise,  $y$ -wise and  $yaw$ -wise states that the vehicle ought to have, that is, each point on the circle serves as a reference to the vehicle. In terms of yaw angle, the longitudinal axis of the vehicle ought to always be tangent to the circle.

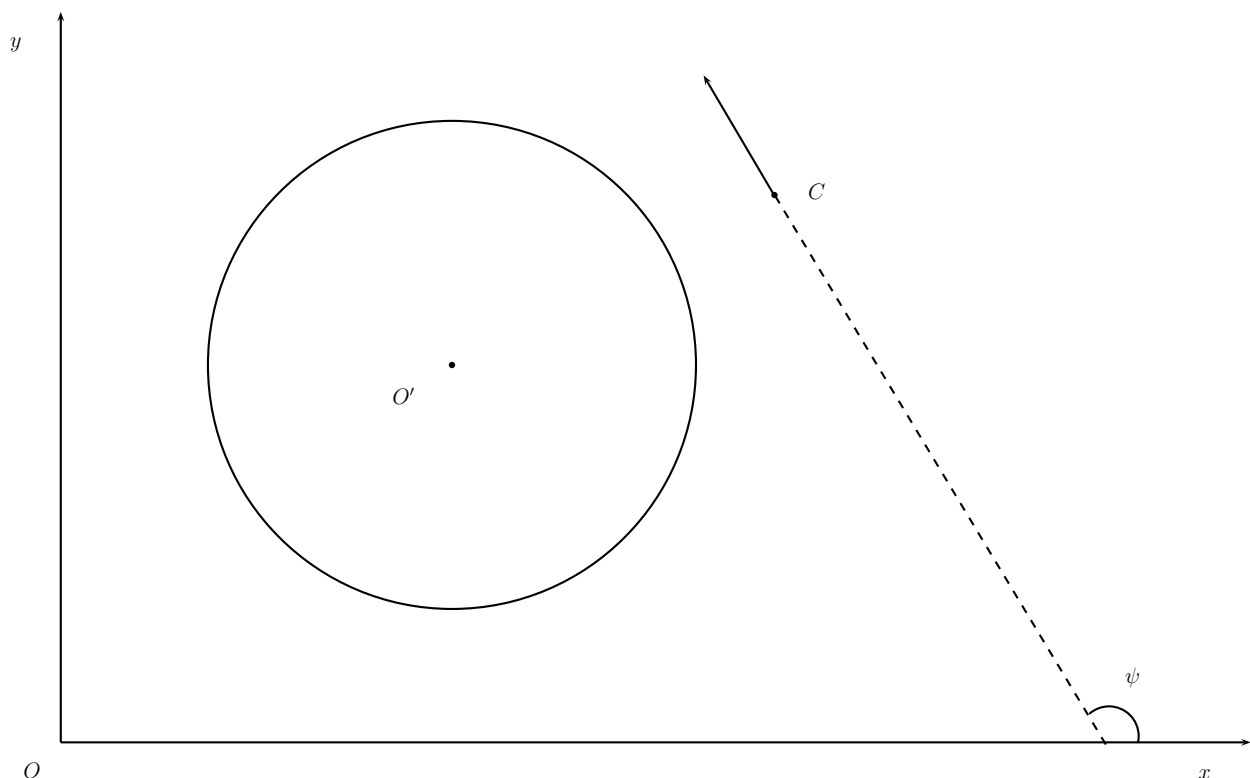


Figure 17

In this setting, since an optimization problem will have to be solved at each time instant  $t$ , the first thing that needs to be identified is the reference pose of the vehicle at each time instant  $t$ . More precisely, since the objective is the minimization of the deviation of the vehicle's trajectory from the circular one, and the framework is that of MPC, we need to identify the sequence of points on the circle that shall act as references while iterating through the prediction equations of the linearized model of the vehicle's behaviour. This task is divided into two sub-tasks: first, we identify the point  $T$  of the circle that lies on the line that is tangent to the circle and that passes through the position of the vehicle. When this point is known, the sequence of  $N - 1$  reference poses can be calculated, given knowledge of the circle's radius and the vehicle's velocity.  $N$  is the horizon length. In the case where the vehicle is in the interior of the circle, no tangent is defined; point  $T$  is then identified as the point that lies on the circle and whose distance

from the vehicle is minimum. The following two sections illustrate the procedures by which the  $N$  reference poses are identified.

### 5.1.1 Finding $T$

Here, we are not concerned with the orientation of the vehicle; its coordinates will only be used as a point to identify the tangent that passes through the position of the vehicle.

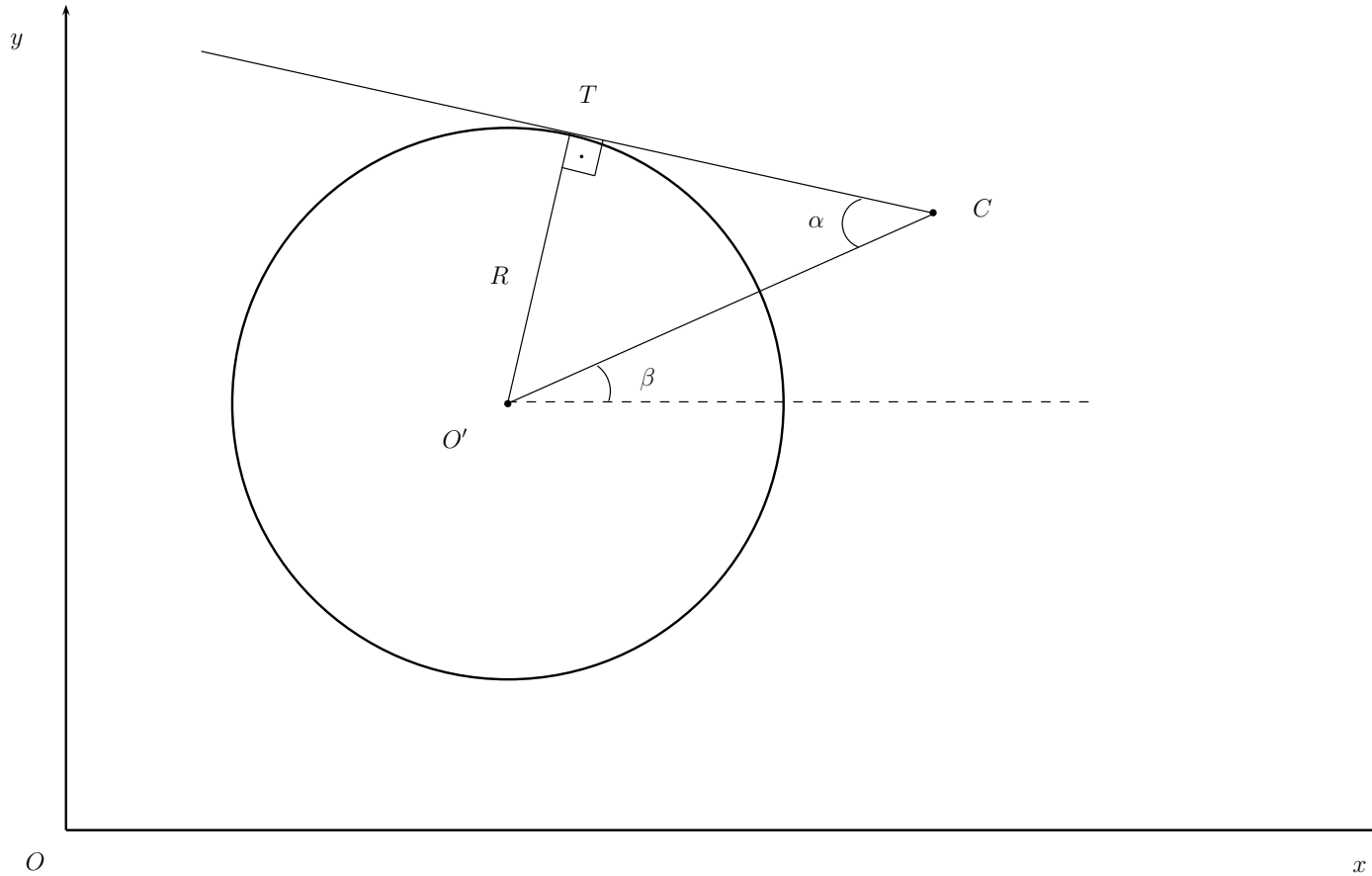


Figure 18

In triangle  $TO'C$ ,  $\angle O'TC$  is right, and

$$\alpha = \sin^{-1} \frac{R}{O'C} \quad (45)$$

while

$$\beta = \tan^{-1} \frac{y_c - y_{O'}}{x_c - x_{O'}} \quad (46)$$

Point  $T$  is then rudimentary to find: it is the point that lies on the circle and is found while rotating by  $\beta + \frac{\pi}{2} - \alpha$  from the  $x$  axis. The coordinates of point  $T$  are

$$x_T = x_{O'} + R \cos \theta_T \quad (47)$$

$$y_T = y_{O'} + R \sin \theta_T \quad (48)$$

$$\theta_T = \beta + \frac{\pi}{2} - \alpha \quad (49)$$

$$(50)$$

The same reasoning applies to when the vehicle is located at every other quadrant. The pose that the vehicle ought to have at point  $T$  of the circle can now be retrieved from the given set of poses. Point  $T$  shall serve as the first reference for the vehicle in the statement of the optimization problem, that is,  $s_T = [x_T, y_T, \psi_T]^T = s_0^{ref}$ . The next task is now to find the next  $N - 1$  reference poses in the circle that the vehicle ought to refer to.

### 5.1.2 Beyond point $T$

The next reference points depend on the velocity of the vehicle. Since its velocity is constant, we know from elementary physics that  $v = \omega R$ , which means that  $\omega = v/R$ , which is known, since the radius of the circle is set by us in advance, and the velocity of the vehicle is measurable. If we denote with  $\theta_T$  the angle that the line passing through  $O'$  and  $T$  makes with the  $x$  axis, with  $\theta_1$  the angle that the line passing through  $O'$  and the first reference point after point  $T$  makes with the  $x$  axis, and  $T_s$  the sampling time of the pose of the vehicle, then

$$\omega = \frac{\Delta \theta}{\Delta t} = \frac{\theta_1 - \theta_T}{T_s} \Leftrightarrow \quad (51)$$

$$\theta_1 = \theta_T + T_s \frac{v}{R} \quad (52)$$

$$(53)$$

In general, the  $k$ -th point in the sequence of the  $N - 1$  reference points will lie at an angle of

$$\theta_k = \theta_T + k T_s \frac{v}{R} \quad (54)$$

$$(55)$$

The coordinates of the  $k$ -th reference point ( $1 \leq k \leq N - 1$ ) are

$$x_k^{ref} = x_{O'} + R \cos \theta_k \quad (56)$$

$$y_k^{ref} = y_{O'} + R \sin \theta_k \quad (57)$$

$$(58)$$

The pose that the vehicle ought to have at each point can be retrieved again from the set of given poses.

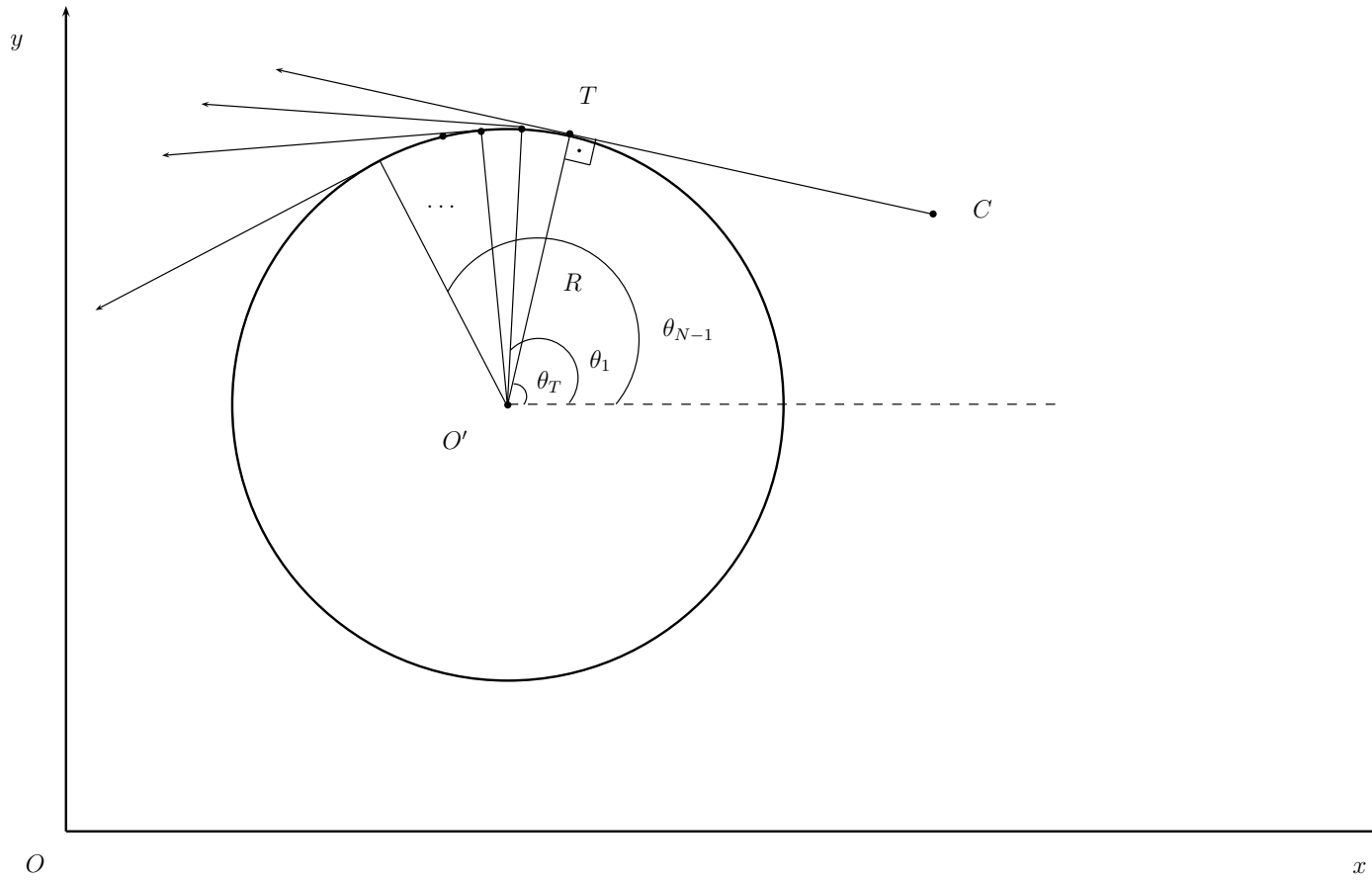


Figure 19

### 5.1.3 Obtaining the linearized kinematic model

The model constitutes the equations of motion of the vehicle, and has three states ( $x$ ,  $y$ , and  $\psi$ ) and one input ( $\delta$ ), since we assume a constant velocity. The equations of the vehicle's motion that are relevant here are

$$\dot{x} = v \cos(\psi + \beta) \quad (59)$$

$$\dot{y} = v \sin(\psi + \beta) \quad (60)$$

$$\dot{\psi} = \frac{v}{l_r} \sin \beta \quad (61)$$

Sampling with a sampling time of  $T_s$  gives

$$x_{k+1} = x_k + T_s v_k \cos(\psi_k + \beta_k) \quad (62)$$

$$y_{k+1} = y_k + T_s v_k \sin(\psi_k + \beta_k) \quad (63)$$

$$\psi_{k+1} = \psi_k + T_s \frac{v}{l_r} \sin \beta_k \quad (64)$$

where

$$\beta_k = \tan^{-1} \left( \frac{l_r}{l_r + l_f} \tan \delta_{k-1} \right) \quad (65)$$

Forming the Jacobians for matrices  $A$ ,  $B$  and evaluating them at time  $t = k$  around the current state  $\psi = \psi_k$ , and  $\delta = \delta_{k-1}$  ( $\delta_k$  is to be determined at time  $k$ ):

$$A = \begin{bmatrix} 1 & 0 & -T_s v_k \sin(\psi_k + \beta_k) \\ 0 & 1 & T_s v_k \cos(\psi_k + \beta_k) \\ 0 & 0 & 1 \end{bmatrix}, \text{ or} \quad (66)$$

$$A = \begin{bmatrix} 1 & 0 & -T_s v_k \sin(\psi_k + \tan^{-1}(l_q \tan \delta_{k-1})) \\ 0 & 1 & T_s v_k \cos(\psi_k + \tan^{-1}(l_q \tan \delta_{k-1})) \\ 0 & 0 & 1 \end{bmatrix} \quad (67)$$

$$B = \begin{bmatrix} -T_s v_k \sin(\psi_k + \beta_k) \frac{l_q}{l_q^2 \sin^2 \delta_{k-1} + \cos^2 \delta_{k-1}} \\ T_s v_k \cos(\psi_k + \beta_k) \frac{l_q}{l_q^2 \sin^2 \delta_{k-1} + \cos^2 \delta_{k-1}} \\ \frac{T_s v_k}{l_r} \cos(\beta_k) \frac{l_q}{l_q^2 \sin^2 \delta_{k-1} + \cos^2 \delta_{k-1}} \end{bmatrix}, \text{ or} \quad (68)$$

$$B = \begin{bmatrix} -T_s v_k \sin(\psi_k + \tan^{-1}(l_q \tan \delta_{k-1})) \frac{l_q}{l_q^2 \sin^2 \delta_{k-1} + \cos^2 \delta_{k-1}} \\ T_s v_k \cos(\psi_k + \tan^{-1}(l_q \tan \delta_{k-1})) \frac{l_q}{l_q^2 \sin^2 \delta_{k-1} + \cos^2 \delta_{k-1}} \\ \frac{T_s v_k}{l_r} \cos(\tan^{-1}(l_q \tan \delta_{k-1})) \frac{l_q}{l_q^2 \sin^2 \delta_{k-1} + \cos^2 \delta_{k-1}} \end{bmatrix} \quad (69)$$

where  $l_q = \frac{l_r}{l_r + l_f}$

Now we can express the linear model as

$$s_{k+1} = A s_k + B u_k \quad (70)$$

where

$$s_k = \begin{bmatrix} x_k \\ y_k \\ \psi_k \end{bmatrix} \quad (71)$$

and

$$u_k = \delta_k \quad (72)$$

However, here there is another option. We can keep the  $A$  and  $B$  matrices constant during the solution of the optimization problem, which means that only one linearization is made (around the current state of the vehicle), or we can solve the problem once with these matrices, extract the sequence of predicted states, and linearize around them. This will result in  $N - 1$  new linearizations around each predicted state of the vehicle,

and hence  $N - 1$  additional  $A_t$  matrices. In the same spirit, we linearize around the corresponding optimal input  $N - 1$  times in total, and we obtain  $N - 1$  additional  $B_t$  matrices.

#### 5.1.4 Stating the optimization problem

We can now form the optimization problem to be solved at time  $t$  as

$$\text{minimize } \sum_{k=0}^{N-1} (s_k - s_k^{ref})^T Q (s_k - s_k^{ref}) + u_k^T R u_k \quad (73)$$

$$\text{subject to } s_{k+1} = A_k s_k + B_k u_k, \text{ where } s_k = [x_k, y_k, \psi_k]^T, u_k = \delta_k \quad (74)$$

$$\delta^{min} \leq \delta_k \leq \delta^{max} \quad (75)$$

$$s_k^{ref} = (x_k^{ref}, y_k^{ref}, \psi_k^{ref}) \quad (76)$$

$$s_0 = (x_t, y_t, \psi_t) \quad (77)$$

where  $A_k$  or  $B_k$  are the Jacobians obtained via linearization around the state of the vehicle at time  $t$ , in which case they are constant across all  $k$ 's, ( $A_k = A$ ,  $B_k = B$ ,  $\forall k$ ) and the problem is solved only once per sampling time; or they are obtained by linearizing around the predicted state of the vehicle, in which case the problem is solved once with  $A_k = A$ ,  $B_k = B$ , and one final time with the variant-time A and B matrices.

## 5.2 Experimental results

The reference circle tested was kept constant, with a radius of  $r = 1.5$  meters, centered around point  $(x_{O'}, y_{O'}) \equiv (0.95, -0.1)$ . In practice, equation 55 was found not to be precise enough for the vehicle to follow the references that the angles  $\theta_k$  dictated: the vehicle could travel in a circular fashion, but the radius of its trajectory was larger than that of the reference trajectory, as can be seen in figure 20. The trajectory of the vehicle is marked with blue, while the reference trajectory is marked with red.

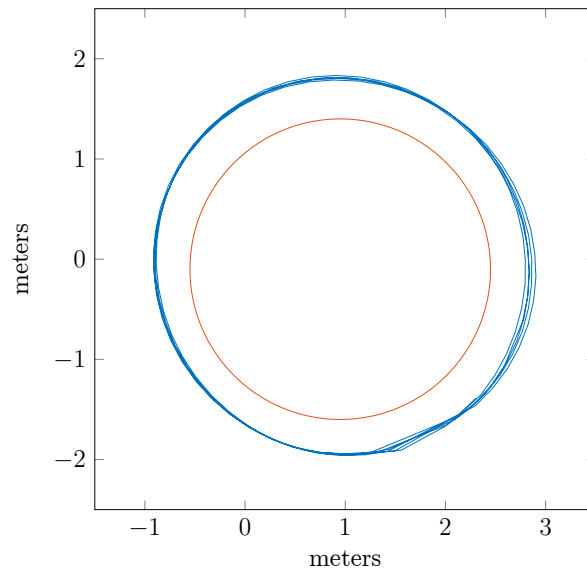


Figure 20: Trajectory of the vehicle in blue and reference trajectory in red, using equation 55 as a means to set the time-varying reference poses.

For this reason, we introduced a corrective factor  $H$ , which is to be considered as an additional factor to be tuned. More concretely, equation 55 was modified as such:

$$\theta_k = \theta_T + kT_s \frac{v}{R} H \quad (78)$$

$$(79)$$

By increasing  $H$ , the references are pushed forward, further along the circle, so that the discrepancy between the radius of the traveled and reference trajectories is minimized. With penalty matrices

$$Q = \begin{bmatrix} 100 & 0 & 0 \\ 0 & 100 & 0 \\ 0 & 0 & 10000 \end{bmatrix}, R = 10 \quad (80)$$

$H = 1.3$  and a horizon length equal to  $N = 2^1$ , we get the results depicted in figures 21 and 22. The vehicle was positioned at  $(1.33, -2.52)$ . Its velocity was kept constant, and its value was set to the minimum that the F1/10 vehicle can do.

These figures illustrate the entire sequence of approaching and maintaining the reference trajectory. The former shows the reference trajectory in red and the trajectory of the vehicle in blue. The latter depicts the displacement error of the vehicle with respect to its trajectory. All measurements are expressed in meters.

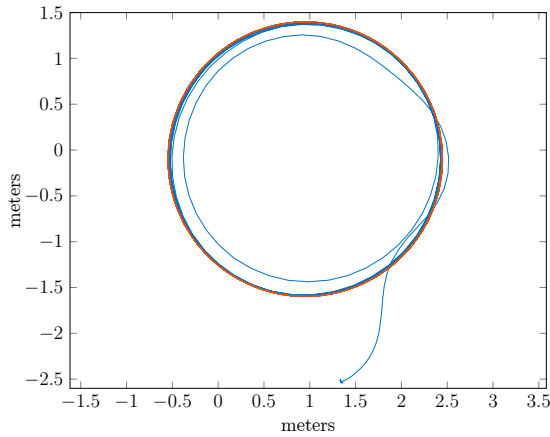


Figure 21: Reference trajectory (red) and trajectory of the vehicle (blue), for the entire sequence of approaching and maintaining the reference trajectory.

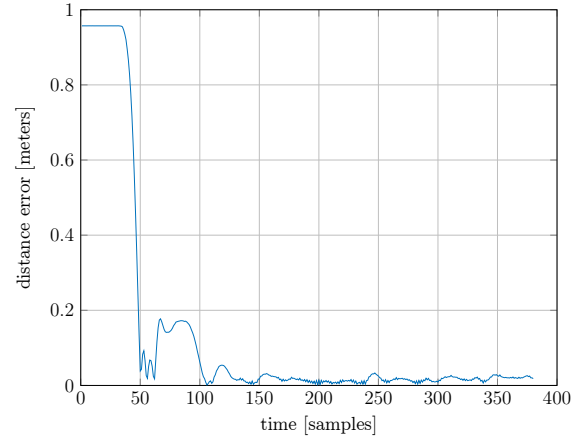


Figure 22: The discrepancy in distance between the trajectory of the vehicle and the reference trajectory for the entire sequence of approaching and maintaining the reference trajectory.

The pairs of figures 23, 24 and 25, 26 feature the breaking down of the entire sequence into the transient phase and the steady state. Notably, in steady state, in this configuration, the error in displacement never exceeds 3.5 cm. Further tuning (namely of the eigenvalues of matrices  $Q, R$  and the value of  $H$ ), and re-evaluation of critical modules that deliver the composite functionality of this ROS package could improve its performance.

<sup>1</sup>in practice we found that references dependent on  $\theta_1$  and  $\theta_2$  give better results than references dependent on  $\theta_0$  and  $\theta_1$ , with  $N = 2$ , or references dependent on  $\theta_{0:2}$  with  $N = 3$

Furthermore, we note that practical experience showed that the higher the ratio  $Q_\psi/Q_{x,y}$ , the closer the vehicle could travel to its intended trajectory. This is because the abiding by the reference orientation is a condition on abiding by the reference position of the car, since the latter is derived directly from the reference orientation minus 90 degrees<sup>2</sup>, and there are no other means of influencing the position of the vehicle other than steering (the effect of  $\beta_k$  rests solely on the steering angle  $\delta_k$ ), since its velocity is kept constant.

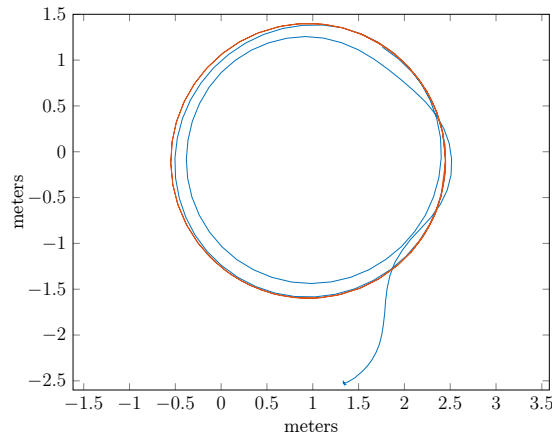


Figure 23: Reference trajectory (red) and trajectory of the vehicle (blue), in the transient phase.

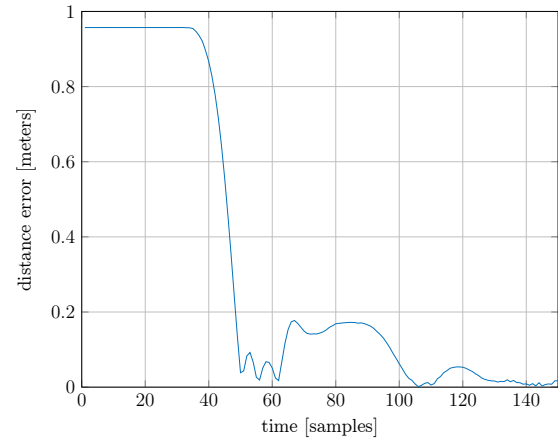


Figure 24: The discrepancy in distance between the trajectory of the vehicle and the reference trajectory in the transient phase.

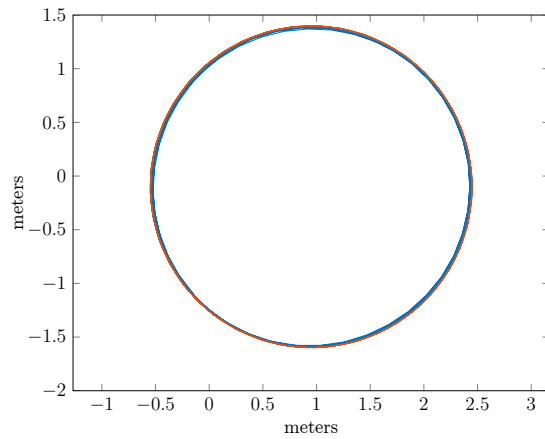


Figure 25: Reference trajectory (red) and trajectory of the vehicle (blue), in steady state.

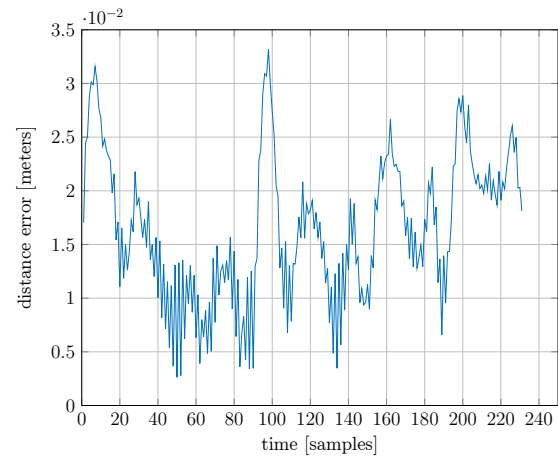


Figure 26: The discrepancy in distance between the trajectory of the vehicle and the reference trajectory in steady state.

Figures 27 and 28 show the result of the optimization process, that is, the steering angle applied to the front wheels of the vehicle during the transient and steady state respectively.

<sup>2</sup> see equations 56 - 57. The reference orientation of the vehicle is implicitly  $\psi_k^{ref} = \theta_k + 90^\circ$



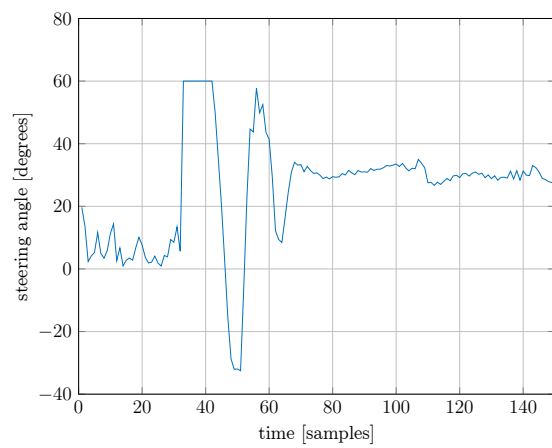


Figure 27: Input through time during the transient phase.

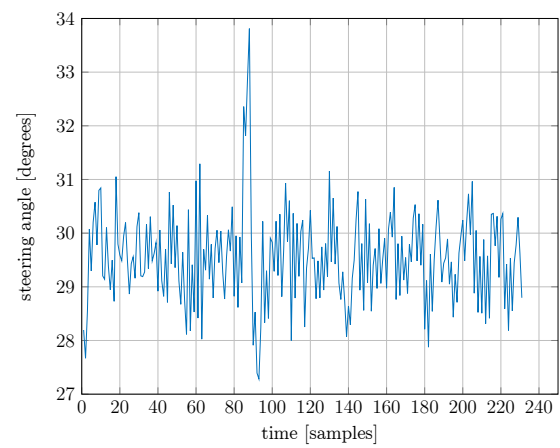


Figure 28: Input through time during steady state.

## 6 On the dynamic model

The kinematic model is tested by a series of specific control signal. By pushing the control signal into the estimation model and comparing the output with the car behavior published by Mocap, the kinematic model can be verified. The result is shown in the figure 29.

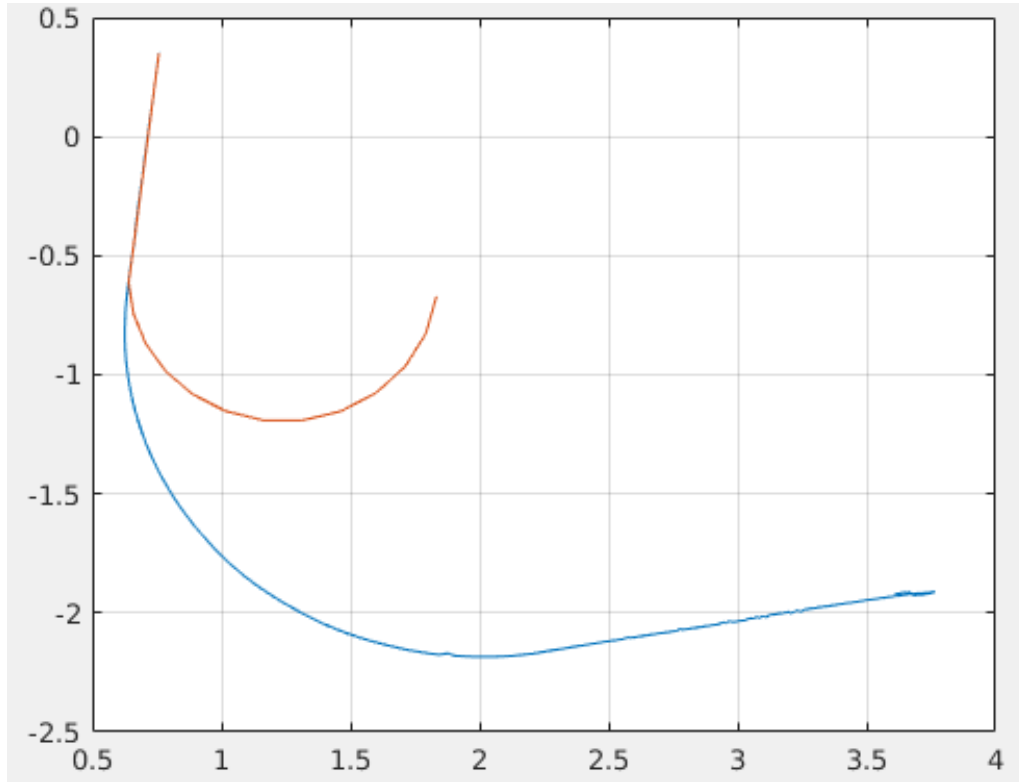


Figure 29: Model and car behavior under a series of specific control signal

As can be seen in the figure 29, red curve represents the model behavior while the blue one is the real car. The most probably reason that the deviation exists is that the car slips when turning.

### 6.1 Dynamic model equations

$$x_g(k+1) = x_g(k) + T_s(v_x(k) \cos(\psi(k)) - v_y(k) \sin(\psi(k)))$$

$$y_g(k+1) = y_g(k) + T_s(v_x(k) \sin(\psi(k)) + v_y(k) \cos(\psi(k)))$$

$$\psi(k+1) = \psi(k) + T_s r(k)$$

$$v_x(k+1) = v_x(k) + T_s/mC_f(\arctan((v_y(k) + r(k)l_f)/v_x(k)) - \delta(k)) \sin(\delta(k)) + T_s r(k)v_y(k)$$

$$v_y(k+1) = v_y(k) - T_s/mC_r \arctan((v_y(k) - r(k)l_r)/v_x(k)) -$$

$$T_s C_f/m(\arctan((v_y(k) + r(k)l_f)/v_x(k)) - \delta(k)) \cos(\delta(k)) - T_s r(k)v_x(k)$$

$$r(k+1) = r(k) - T_s l_f C_f/J_z \cos(\delta(k))(\arctan((v_y(k) + r(k)l_f)/v_x(k)) - \delta(k)) +$$

$$T_s C_r/J_z \arctan((v_y(k) - r(k)l_r)/v_x(k))$$

$$v(k+1) = v(k) + T_s(v_r \text{ef}(k) - \sqrt{v_x(k)^2 + v_y(k)^2})/\tau$$

The  $v_x, v_y$  are the velocity component at local coordinate, while  $x_g, y_g$  are the position component at global coordinate.

There are three parameters in the model need to be defined i.e. inertia of the car around z-direction  $J_z$ , cornering stiffness for front and rear wheels  $C_f, C_r$ . The estimation of these will be described next.

## 6.2 Parameter estimation

Here we use similar method to the one used in time-constant estimation. By putting certain series of input signals, both velocity and steering angle, the Mocap system generate the corresponding position signals as car running. Meanwhile in Matlab we generate the estimated position signals with the dynamic model given the same series of input. The next step is to use Matlab Will do it with Matlab function Simulink Design Optimization toolbox to find the optimize solutions of the problem in

$$\min_{J_z, C_f, C_r} estimate\_error = (measurement - estimate\_position)^2 \quad (81)$$

The aim is to generate a qualified dynamic model which will be used as the inner model of the MPC controller, in order to drive the car as fast as possible. But due to the time limitation, we have not manage to achieve some satisfying parameters.

## 7 Conclusion

This report illustrated the theoretical approaches, theoretical and practical solutions, and results to three control problems. These problems, although seemingly simple, required tailored solutions depending on the nature of their respective available resources (e.g. for localisation), and solution regimes (e.g. predictive control). Practical experience showed us that the apparent simplicity of problems does not go hand-in-hand with the difficulty of their solutions: the real world is not sterile like a simulation environment. In light of the discrepancy between the performance of purely theoretically sound solutions and their expected performance, we manipulated minor or major parts of these solutions and tweaked others, so as to gain an understanding of the hidden dynamics and implications present in the real world, and exploit it in order to reduce the aforementioned discrepancies to a level that we deemed to be tolerable.

In the problem of approaching and maintaining the centerline of a virtual lane, our solutions made it possible for the vehicle to execute this task with success. The predictive control approach featured a slower settling time than the PID one, however the former proved to be more robust than the latter. In the more difficult problem of approaching and maintaining the trajectory of a circumference of a circle with a radius of 1.5 m, the vehicle's displacement error does not exceed 3.5 cm.

Lastly, the length of this report does not meet the 10-page requirement. To have been so, that would mean that its quality would have been worse. The report is written in a way so as to be read fluently, comprehensively and concisely: the length of the report is proportional to the joint difficulty of the problems tackled and the representation of their solution. The report uses signposts to divide and link all the separate sub-problems and the approach taken to handle them in order to order meaning and increase comprehension. Furthermore, in the spirit of, and interest in providing a solid documentation for future potential successors of our work, we deemed it would be best to combine all documentation and methodical approaches in one document. This we think will augment clarity and set a foundation for understanding the handling of dynamics of a F1/10 (or other similar) vehicle.